Cell Reports
Report

Cell PRESS
Open ACCESS

Obesity Promotes Liver Carcinogenesis via Mcl-1 Stabilization Independent of IL-6Rα Signaling

Sabine Gruber,[1] Beate K. Straub,[2] P. Justus Ackermann,[1] Claudia M. Wunderlich,[1] Jan Mauer,[1] Jens M. Seeger,[3] Hildegard Büning,[4] Lukas Heukamp,[5] Hamid Kashkar,[3] Peter Schirmacher,[2] Jens C. Brüning,[1] and F. Thomas Wunderlich[1,*]

[1]Max Planck Institute for Neurological Research Cologne; Institute for Genetics, University of Cologne; Cologne Excellence Cluster on Cellular Stress Responses in Aging-associated Diseases (CECAD); Center for Molecular Medicine Cologne (CMMC); Center for Endocrinology, Diabetes and Preventive Medicine (CEDP) Cologne, 50931 Cologne, Germany
[2]Institute of Pathology, University Hospital Heidelberg, 69120 Heidelberg, Germany
[3]Institute for Medical Microbiology, Immunology and Hygiene, University of Cologne; CMMC; CECAD; 50937 Cologne, Germany
[4]Department I of Internal Medicine, University of Cologne; CMMC; 50935 Cologne, Germany
[5]Institute of Pathology, University of Cologne, 50937 Cologne, Germany
*Correspondence: thomas.wunderlich@uni-koeln.de
http://dx.doi.org/10.1016/j.celrep.2013.07.023
This is an open-access article distributed under the terms of the Creative Commons Attribution-NonCommercial-No Derivative Works License, which permits non-commercial use, distribution, and reproduction in any medium, provided the original author and source are credited.

SUMMARY

Obesity increases the incidence of hepatocellular carcinoma (HCC) development in part through the activation of obesity-associated proinflammatory signaling. Here, we show that in lean mice, abrogation of IL-6Rα signaling protects against diethylnitrosamine (DEN)-induced HCC development. HCC protection occurs via Mcl-1 destabilization, thus promoting hepatocyte apoptosis. IL-6 regulates Mcl-1 stability via the inhibition of PP-1α expression, promoting GSK-3β inactivation. In addition, IL-6 suppresses expression of the Mcl-1 E3 ligase (Mule). Consequently, IL-6Rα deficiency activates PP-1α and Mule expression, resulting in increased Mcl-1 turnover and protection against HCC development. In contrast, in obesity, inhibition of PP-1α and Mule expression, leading to Mcl-1 stabilization, occurs independently of IL-6 signaling. Collectively, this study provides evidence that obesity inhibits hepatocyte apoptosis through Mcl-1 stabilization independent of IL-6 signaling, thus promoting liver carcinogenesis.

INTRODUCTION

Epidemiological studies have identified obesity as a major risk factor for several cancer entities (Bianchini et al., 2002; Calle and Kaaks, 2004), among which hepatocellular carcinoma (HCC) exhibited the strongest obesity-associated increase in tumor incidence (Calle et al., 2003). Thus, the obesity-associated increase in HCC development may gain substantial clinical significance in light of the steadily increasing incidence of obesity in westernized societies (Ford and Mokdad, 2008). Obesity is known to result in a chronic low-grade proinflammatory state as a consequence of immune cells infiltrating white adipose tissue (WAT) and liver. This in turn results in elevated circulating concentrations of cytokines such as tumor necrosis factor alpha (TNF-α) and interleukin-6 (IL-6) (Nishimura et al., 2009; Xu et al., 2003; Hotamisligil, 2006). Therefore, obesity-associated inflammation provides a potential link between obesity and liver carcinogenesis. Accordingly, studying TNF-α- and IL-6-evoked signaling pathways that are upregulated both in obesity and during HCC development has provided new insights into the pathogenesis of these disorders (Park et al., 2010). Impairment of TNF-α-induced NF-κB signaling in liver parenchymal cells through liver-specific *NEMO* deficiency in $NEMO^{L\text{-}KO}$ mice causes spontaneous liver tumorigenesis (Luedde et al., 2007) that is further aggravated when these animals are exposed to high fat diet (HFD)-induced obesity (Wunderlich et al., 2008). Further detailed analyses showed that obese $NEMO^{L\text{-}KO}$ mice sequentially developed liver inflammation with a concomitant increase of IL-6, which eventually contributes to the development of liver tumors. Importantly, both genetically and diet-induced obesity are known to aggravate liver carcinogenesis in the DEN-induced HCC model, and obesity-induced enhancement of liver carcinogenesis is dependent on TNF-α signal transduction (Park et al., 2010). In addition, this study also showed that liver carcinogenesis in lean and obese mice is IL-6 dependent (Park et al., 2010). Taken together, these findings provide strong evidence that obesity increases HCC incidence by inducing inflammatory conditions that involve TNF-α and IL-6. Moreover, previous studies have also shown that obesity decreases hepatocyte death (Park et al., 2010). However, the exact underlying molecular mechanisms and their contribution in both IL-6- and obesity-induced HCC development still remain to be elucidated.

Here, we show that interleukin-6 receptor α (*IL-6Rα*) deficiency protects against DEN-induced HCC development in lean mice, a

finding that is consistent with the previously described IL-6 dependency of liver tumor development (Naugler et al., 2007). Moreover, in line with previous observations, HFD-induced obesity aggravates DEN-induced HCC development and progression compared to normal chow diet (NCD)-fed mice (Park et al., 2010). Surprisingly, this HFD-induced obesity abrogates the protective effect of *IL-6Rα* deficiency on HCC development. We show that IL-6 and obesity promote HCC progression through stabilization of the Bcl-2 family member Mcl-1 that in turn inhibits apoptosis of damaged hepatocytes and contributes to malignant transformation and HCC progression. Mcl-1 stabilization in lean mice was found to occur as a consequence of IL-6-induced glycogen synthase kinase 3 β (GSK-3β) inactivation as well as reduced *Mule* expression, whereas in obese animals this mechanism occurred independently of IL-6 signaling. Thus, this study has strong implications for current translational research on HCC therapeutic strategies aiming at reactivating the mitochondrial apoptotic pathway under inflammatory and obese conditions.

RESULTS

Obesity Increases Basal Hepatic Stat-3 Activation and Impairs Acute IL-6 Responsiveness

IL-6 initiates downstream signaling by binding to the IL-6R consisting of two subunits of the signal-transducing β chain of the receptor that is also used by a cohort of other IL-6-type cytokines and one subunit of the IL-6Rα chain that confers IL-6 binding and thus specificity to the receptor complex (Heinrich et al., 2003). IL-6R activation results in multiple downstream signaling events in the liver such as activation of the JAK/Stat-3 and MAPK/ERK pathways, whereas phosphorylation of Stat-3 appeared already 30 min after IL-6 injection and progressively declined thereafter (Figure S1A). However, IL-6 injection did not activate hepatic JNK phosphorylation in our control mice (Figure S1A). Next, in a dose response of IL-6 in lean control mice, IL-6-induced Stat-3 activation in liver was already detected upon injection of 3 ng IL-6 per gram body weight (BW), which was dose-dependently increased when 30 and 300 ng IL-6/g BW were applied (Figure S1B). Surprisingly, while injection of 50 ng IL-6/g BW induced a prominent hepatic activation of Stat-3 in lean mice, this response was dramatically blunted when control mice were obese owing to the exposure to HFD (Figures S1C and S1D). Noteworthy, in the basal state, obese livers demonstrated increased Stat-3 activation compared to lean mice (Figure S1C). Collectively, these experiments demonstrate that obesity increases basal Stat-3 activation and impairs acute responsiveness to IL-6, presumably as a result of the low-grade proinflammatory state under obese conditions.

To study the role of IL-6Rα-dependent signaling in obesity-associated liver carcinogenesis, we crossed IL-6Rα^{FL} mice (Wunderlich et al., 2010) to deleter Cre mice and intercrossed offspring to yield IL-6Rα^{KO} mice (Wunderlich et al., 2012). Quantitative PCR (qPCR) of liver complementary DNA (cDNA) of IL-6Rα^{FL} control and IL-6Rα^{KO} mice revealed the absence of *IL-6Rα* expression in IL-6Rα^{KO} mice (Figure S1E). Accordingly, IL-6 was unable to induce hepatic Stat-3 phosphorylation in IL-6Rα^{KO} mice, whereas CNTF potently induced Stat-3 activation in these animals (Figure S1F). In contrast, hepatic Stat-3 activation occurred to a similar extent in both control and *IL-6*-deficient mice when exposed to IL-6 or CNTF (Figure S1F). In addition, LPS was observed to potently induce Stat-3 and JNK phosphorylation in control mice but failed to activate Stat-3 in *IL-6Rα*- and *IL-6*-deficient mice, thereby indicating that LPS-induced Stat-3 activation is mainly derived from IL-6/IL-6Rα signaling (Figure S1F). Thus, our experiments revealed successful inactivation of IL-6-evoked signaling in IL-6Rα^{KO} mice while the responsiveness to alternative IL-6Rα-independent gp130 cytokines such as CNTF remained unaltered.

HFD Causes Obesity in Control and IL-6Rα^{KO} Mice in the DEN-Induced HCC Model

HCC represents a classical inflammation-induced cancer entity, the development of which is significantly enhanced under obese conditions (Park et al., 2010; Wunderlich et al., 2008). To investigate whether *IL-6Rα* deficiency affects HCC development under normal and obese conditions, we injected male IL-6Rα^{FL} control and IL-6Rα^{KO} mice with DEN at 15 days of age and separated these animals after weaning in cohorts fed on either an NCD or HFD. Importantly, HFD significantly increased body weight (Figure S2A), impaired glucose tolerance (Figure S2B), and increased circulating concentrations of insulin, TNF-α, and IL-6 in sera of control and IL-6Rα^{KO} mice (Figure S2C–S2E). However, *IL-6Rα* deficiency did not affect HFD-induced obesity or obesity-induced insulin resistance and inflammation. Alternative modulation of IL-6 type cytokine signaling by *trans*-signaling of soluble receptors such as sIL-6Rα and sgp130 might also contribute to obesity-induced inflammation. However, while consistently in *IL-6Rα*-deficient mice the sIL-6Rα was at the lowest detection level but unchanged between control mice on both diets, sgp130 was reduced in obese IL-6Rα^{KO} mice compared to lean but comparable to control animals (Figures S2F and S2G). HFD feeding was observed to induce hepatocyte steatosis that can sequentially lead to the development of liver damage and steatohepatitis that in turn might result in HCC development. As an indirect indicator of liver damage, the activity of the liver aspartate transaminase AST was not significantly different in the serum of control and IL-6Rα^{KO} mice fed on either an NCD or HFD (Figure S2H). Oil red O staining of liver sections of the four different groups of mice revealed increased hepatic fat stores in mice exposed to HFD feeding in both control and IL-6Rα^{KO} mice, although lipid accumulation was comparable between the two genotypes (Figure S2I). Taken together, our data demonstrate that HFD exposure causes similar levels of obesity in both control and IL-6Rα^{KO} mice upon DEN induction.

Obesity Promotes HCC Development and Abrogates the Effect of *IL-6Rα* Deficiency on liver Carcinogenesis

We next analyzed tumor development in 8-month-old DEN-treated control and IL-6Rα^{KO} mice that had been exposed to either an NCD or HFD (Figure 1A). Male control NCD-fed mice developed approximately 30 macroscopically visible liver tumors (Figure 1B), of which 66% were smaller than 2 mm (Figure 1C) and 33% reached a size of more than 2 mm (Figure 1D). Similar to *IL-6*-deficient mice (Naugler et al., 2007), we found that *IL-6Rα* deficiency potently protected mice from developing

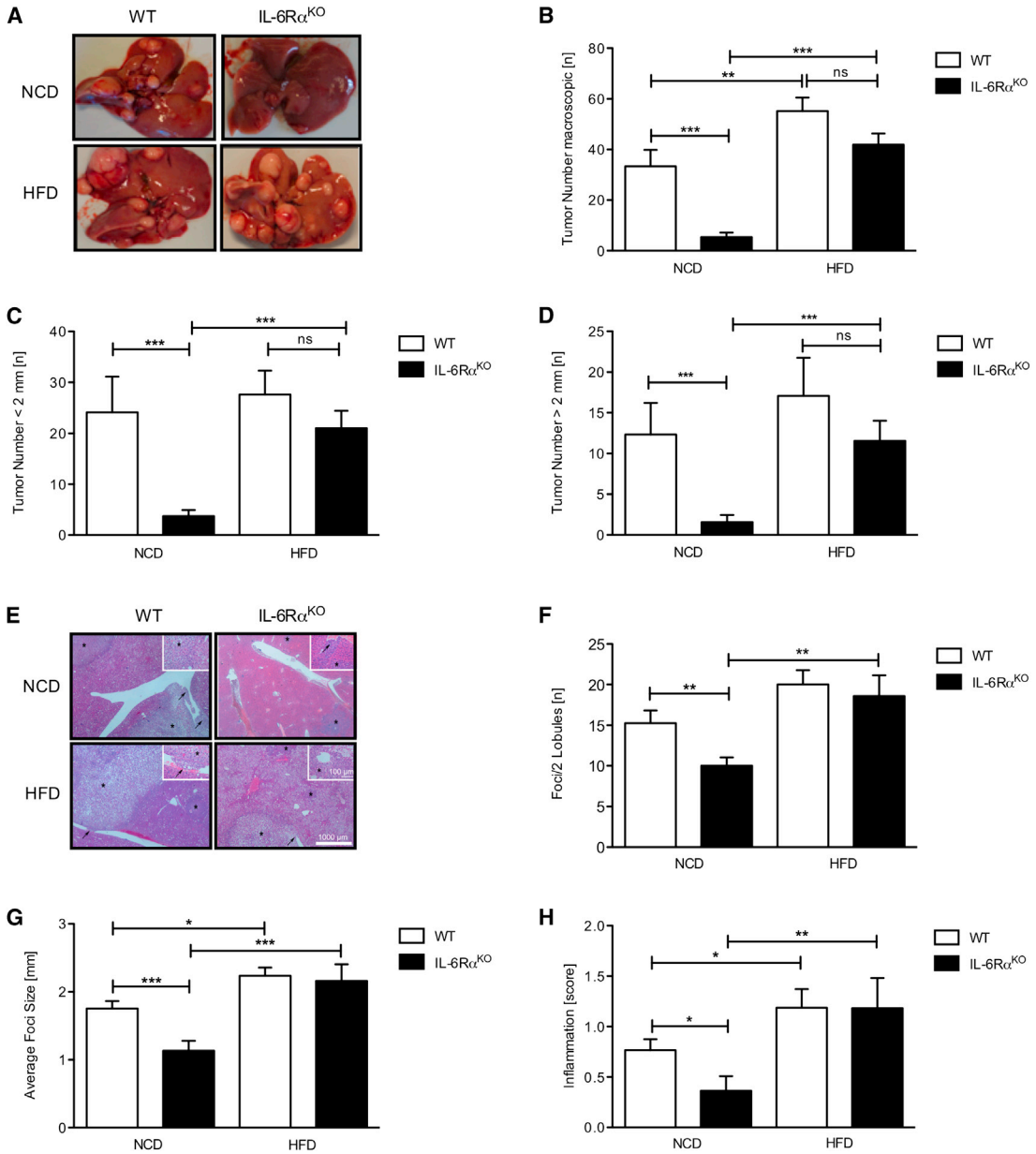

Figure 1. Obesity Compensates for *IL-6Rα* Deficiency in HCC Pathogenesis

(A) Livers of 8-month-old (8-mo) control and IL-6Rα^{KO} mice injected with 25 mg/kg DEN at 15 days of age.

(B) Quantitation of macroscopic tumor multiplicity determined by visual inspection in DEN-injected 8-month-old control and IL-6Rα^{KO} mice (n = 15).

(C and D) Enumeration of tumor number for < 2 mm (C) and > 2 mm (D) as determined by visual inspection of DEN-injected 8-mo control and IL-6Rα^{KO} mice (n = 15).

(E) Hematoxylin/eosin-stained sections of livers from DEN-injected 8-mo control and IL-6Rα^{KO} mice. Asterisks indicate tumor foci; arrows indicate tumorous blood vessel infiltrates.

(F) Quantitation of tumor number per two lobules counted on liver sections from 8-mo control and IL-6Rα^{KO} mice (n = 15).

(G) Quantitation of tumor size measured in the big liver lobe of DEN-injected 8-mo control and IL-6Rα^{KO} mice (n = 15).

(H) Quantitation of inflammation measured in the big liver lobe of DEN-injected 8-mo control and IL-6Rα^{KO} mice. 1 = mild inflammation (mild portal inflammation, three to five single cell necrosis, no grouped necrosis); 2 = moderate inflammation (moderate portal inflammation, six to nine single cell necrosis, one grouped necrosis); 3 = severe inflammation (severe portal inflammation, more than ten single cell necrosis, more than one grouped necrosis) (n = 15).

Displayed values are means ± SEM; *p ≤ 0.05, **p ≤ 0.01, ***p ≤ 0.001 versus control. See also Figure S1.

DEN-induced HCC when fed on an NCD (Figures 1A–1D). In line with previous experiments, obesity increased tumor burden to approximately 50 tumors in control mice (Figures 1A and 1B) (Park et al., 2010). Strikingly, however, when IL-6Rα^{KO} mice were fed a HFD, the protective effect of *IL-6Rα* deficiency on HCC development was abrogated as DEN treatment induced

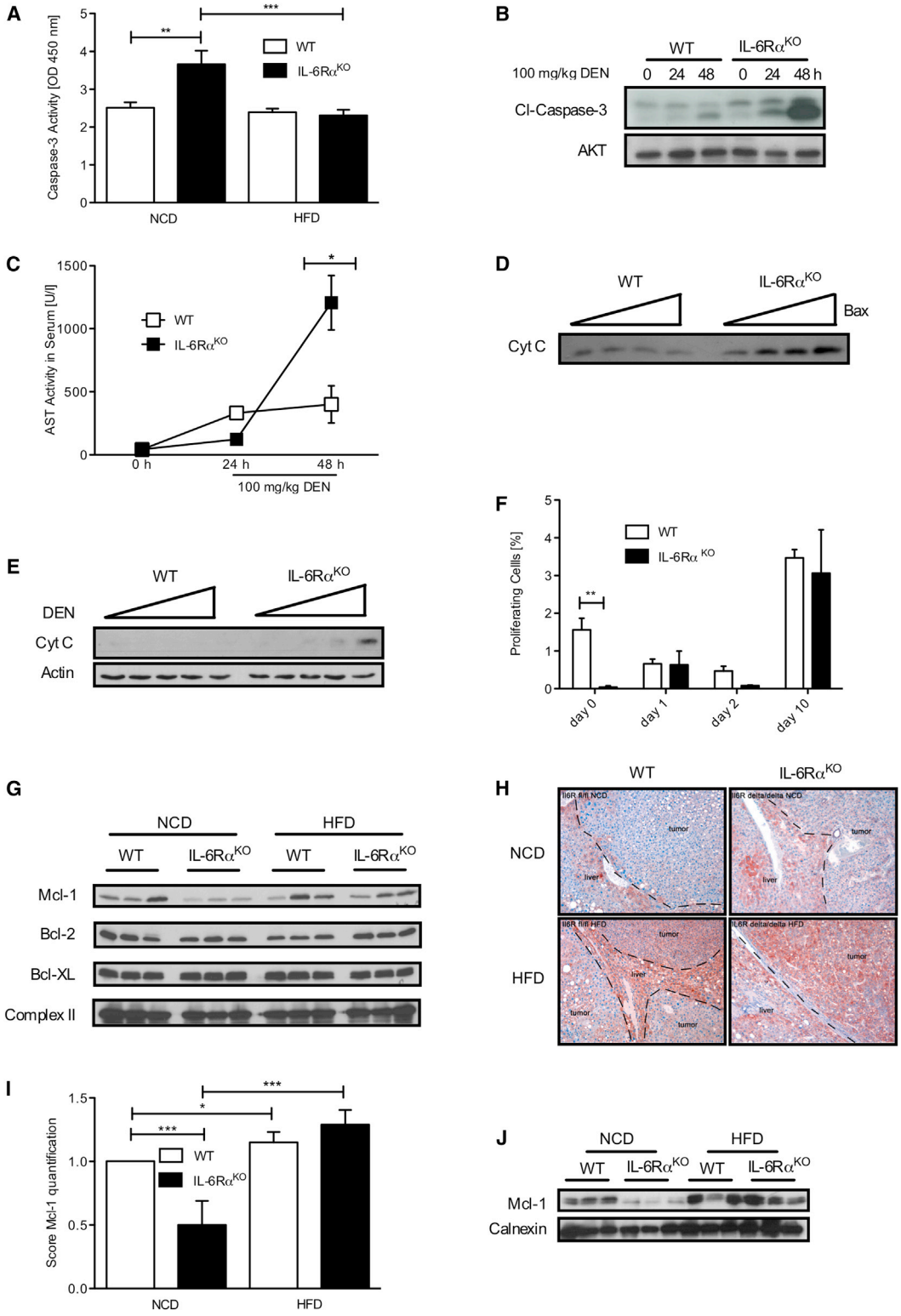

Figure 2. Obesity and IL-6 Accelerate HCC Pathogenesis through Mcl-1 Stabilization

(A) Determination of caspase-3 activity using an ELISA-based assay on liver lysates from DEN-injected 8-mo control and IL-6Rα^{KO} mice (n = 5).

(B) Western blot analysis using cleaved caspase-3 and AKT antibodies on liver tissue from 8-week-old (8-wk) control and IL-6Rα^{KO} mice fed on an NCD and sacrificed at the indicated time points after a 100 mg/kg DEN injection.

(legend continued on next page)

significantly higher tumor numbers in these mice comparable to control mice with an HFD (Figures 1A and 1B). Histological investigation of hematoxylin and eosin-stained liver sections (Figure 1E) confirmed that NCD-fed IL-6Rα^{KO} mice had significantly decreased number and size of HCC foci (Figures 1F and 1G) when compared to NCD-fed control mice, although this difference was not as large as observed upon macroscopic inspection. Strikingly, HFD feeding restored the carcinogenic capability of DEN in IL-6Rα^{KO} animals as the number and size of HCC foci increased to the same extent in control mice and IL-6Rα^{KO} mice when exposed to an HFD (Figures 1F and 1G). Moreover, the extent of inflammation as assessed by quantitation of infiltrating immune cells and necrosis of hepatocytes was significantly reduced in livers of IL-6Rα^{KO} mice compared to control mice exposed to an NCD (Figure 1H). In contrast, HFD feeding significantly increased liver inflammation of both control and IL-6Rα^{KO} animals (Figure 1H). While it is certainly not clear which factor in obesity compensates for *IL-6Rα* deficiency in HCC development, evidently another IL-6-type cytokine or receptor might account for this observation, as inactivation of *gp130* in hepatocytes protected against DEN-induced HCC development even under obese conditions (Figure S2J). However, determination of IL-6-type cytokine and receptor expression levels in tumor livers of control and *IL-6Rα*-deficient animals under both dietary conditions failed to directly clarify this point, which needs further investigation (Figures S2K–S2N). Taken together, these data demonstrate that obesity promotes HCC development and progression and renders tumor development independently of IL-6Rα signaling, thus abrogating the protective function of *IL-6Rα* deficiency under NCD conditions.

Obesity and IL-6 Increase HCC Development through the Inhibition of Mitochondrial Apoptosis

IL-6 is a potent survival signal in hepatocytes, and deletion of its receptor may thus affect hepatocyte death signaling and survival. Therefore, we examined apoptosis in the livers of the different cohorts of mice by determining the presence of active caspase-3. Increased caspase-3 activation was detected in liver lysates derived from NCD-fed IL-6Rα^{KO} mice upon DEN treatment, whereas significantly decreased caspase 3 activation was detected in HFD-fed IL-6Rα^{KO} mice (Figure 2A). In line with this observation, upon a single DEN injection, caspase-3 cleavage/activation dramatically increased in livers of IL-6Rα^{KO} mice (Figure 2B). These data were further substantiated by the finding that AST activity was elevated in sera of IL-6Rα^{KO} mice upon acute DEN injection, another strong indicator of liver damage (Figure 2C). Mitochondria represent a central sensory organelle that can respond to DNA damage by mitochondrial outer membrane permeabilization, a process that is tightly regulated by Bcl-2 protein family members (Brunelle and Letai, 2009). To experimentally address whether increased DEN-induced apoptosis in IL-6Rα^{KO} mice is a consequence of enhanced mitochondrial apoptotic response, freshly isolated mitochondria from livers of naive control and IL-6Rα^{KO} mice were incubated with increasing amounts of recombinant Bax protein and the release of mitochondrial cytochrome *c* was measured by western blot analysis (Figure 2D). These analyses demonstrated that mitochondria derived from the livers of IL-6Rα^{KO} mice were more susceptible to recombinant Bax as demonstrated by the increased appearance of cytosolic cytochrome *c* (Figure 2D). Consistently, *IL-6Rα*-deficient hepatocytes demonstrated concentration-dependent cytosolic cytochrome *c* levels in response to DEN (Figure 2E). Collectively, these experiments demonstrate increased hepatic apoptosis sensitivity of lean *IL-6Rα*-deficient mice. Hepatocyte apoptosis has been shown to result in compensatory proliferation of adjacent hepatocytes to cause HCC development (Bisgaard and Thorgeirsson, 1996). Thus, we compared proliferation of hepatocytes in response to DEN-induced apoptosis in lean control and IL-6Rα^{KO} mice (Figure 2F). While hepatocyte proliferation was significantly reduced in *IL-6Rα*-deficient animals without DEN injection, DEN-induced compensatory proliferation of hepatocytes was comparable between control and IL-6Rα^{KO} mice as examined through quantitation of Ki67-positive hepatocytes in livers of these mice. Thus, increased apoptosis sensitivity, but not impairments in compensatory proliferation, might confer the protection of lean *IL-6Rα*-deficient mice against DEN-induced HCC development. The balance between anti- and proapoptotic members of the Bcl-2 protein family regulates mitochondrial outer membrane permeabilization and the efflux of cytochrome *c* in response to cellular damage (Brunelle and Letai, 2009). The presence of the antiapoptotic Bcl-2 protein family members Mcl-1, Bcl-2, and Bcl-XL at mitochondria has been shown to prevent cytochrome *c* release. Western blot analysis of mitochondrial extracts derived from tumor livers of the different cohorts of mice revealed a reduced mitochondrial level of Mcl-1 in NCD-fed IL-6Rα^{KO} mice (Figure 2G). Interestingly, upon HFD feeding, mitochondrial Mcl-1 protein levels were restored to comparable levels in both control and *IL-6Rα*-deficient animals (Figure 2G).

(C) Determination of serum AST activity to assess liver damage in 8-wk control and IL-6Rα^{KO} mice fed on an NCD and sacrificed at the indicated time points after a 100 mg/kg DEN injection (n = 6).
(D) Cytochrome *c* release of isolated mitochondria after treatment with increasing concentrations of recombinant Bax. Mitochondria were isolated from naive 8-wk control and IL-6Rα^{KO} mice fed an NCD.
(E) Western blot analysis using cytochrome *c* and actin antibodies of cytosolic extracts from primary hepatocytes isolated from 8-wk control and IL-6Rα^{KO} mice that were treated with 0, 0.25, 0.5, 1, and 5 mM DEN for 48 hr in culture.
(F) Quantitation of proliferating Ki67-positive hepatocytes in liver sections from 8-wk control and IL-6Rα^{KO} mice sacrificed at the indicated time points upon injection of 100 mg/kg DEN (n = 3).
(G) Western blot analysis using Mcl-1, Bcl-2, Bcl-XL, and Complex II antibodies on isolated mitochondria from DEN-injected 8-mo control and IL-6Rα^{KO} mice.
(H) Representative Mcl-1-stained sections of livers from DEN-injected 8-mo control and IL-6Rα^{KO} mice. Dashed lines discriminate tumor and normal liver tissue.
(I) Quantitation of Mcl-1 in tumors of the big liver lobe from DEN-injected 8-mo control and IL-6Rα^{KO} mice. 0 = no Mcl-1, 1 = low Mcl-1, 2 = high Mcl-1.
(J) Western blot analysis using Mcl-1 and Calnexin antibodies on isolated tumors from DEN-injected 8-mo control and IL-6Rα^{KO} mice.
Displayed values are means ± SEM; *p ≤ 0.05, **p ≤ 0.01, ***p ≤ 0.001 versus control. See also Figure S2.

Notably, protein levels of Bcl-2 and Bcl-XL were not altered between diets and genotypes. Consistent with these data, immunohistochemistry of mouse liver sections demonstrated that HFD significantly increased Mcl-1 protein abundance in the tumors independently of IL-6Rα signaling (Figures 2H and 2I). The tumor-associated *Mcl-1* expression was further analyzed in dissected HCCs from livers of the different groups of mice in western blot analysis, demonstrating that Mcl-1 protein was decreased in HCCs of lean *IL-6Rα*-deficient mice compared to control tumors, while HFD increased Mcl-1 protein in HCCs of control as well as IL-6Rα^{KO} mice (Figures 2J and S2O). Strikingly, qPCR analyses of liver cDNA of the four different groups of mice revealed that the transcriptional level of *Mcl-1* was largely unaltered (Figure S2P), suggesting that the reduced Mcl-1 content of mitochondria of IL-6Rα^{KO} mice might be caused by a posttranslational regulatory mechanism. Taken together, these experiments demonstrate that under NCD conditions, loss of IL-6 signaling sensitizes hepatocytes to damage-induced apoptosis. In turn, apoptosis may contribute to the attrition of damaged cells with an enhanced malignant potential and thus protects from tumor development. However, under HFD conditions, hepatocyte apoptosis is inhibited, even in the absence of IL-6Rα signaling, presumably by increased protein abundance of the antiapoptotic Bcl-2 protein family member Mcl-1, especially within the tumor lesions.

GSK-3β Inhibition Stabilizes Mcl-1 under Obese Conditions in HCC Development

The Mcl-1 protein comprises an N-terminal PEST domain that is responsible for its relatively short half-life. Among the numerous protein kinases that have been implicated in the regulation of Mcl-1, GSK-3β is known to play a pivotal role in controlling Mcl-1 protein stability (Maurer et al., 2006). GSK-3β is a serine/threonine protein kinase that unlike most other protein kinases is constantly active, but becomes inactivated upon phosphorylation at serine residue 9 (S9). Interestingly, inactivation of GSK-3β via phosphorylation at S9 increases stabilization and accumulation of Mcl-1 protein and thus prevents apoptosis (Ding et al., 2007). To address the role of GSK-3β action in Mcl-1 protein stability during HCC development, we analyzed GSK-3β phosphorylation in the livers of DEN-treated control and IL-6Rα^{KO} mice on either an NCD or HFD (Figures 3A and S3A). Remarkably, GSK-3β was less phosphorylated at S9 and thus more active in livers of IL-6Rα^{KO} mice on an NCD (Figures 3A, S3A, and S3B), whereas total GSK-3β levels were unaltered (Figure S3C). Interestingly, GSK-3β S9 phosphorylation was reconstituted and Mcl-1 levels were increased in livers of IL-6Rα^{KO} mice when exposed to HFD feeding (Figures 3A and S3A). Consistent with these observations, direct assessment of GSK-3β kinase activity showed that in livers of IL-6Rα^{KO} mice on an NCD, but not on HFD, GSK-3β activity was significantly enhanced (Figure 3B). Active GSK-3β has been previously demonstrated to regulate apoptosis through expression of the BH3-only member *PUMA* that antagonizes Mcl-1 to sensitize for apoptosis (Charvet et al., 2011). Consistently, *PUMA* expression was 2-fold increased in tumor livers of IL-6Rα^{KO} mice but restored under obese conditions (Figure S3D). Of note, expression of the other BH3 only family member *NOXA* was unchanged between genotypes and diets (Figure S3E). We next examined whether inactivation of GSK-3β is a downstream event of IL-6 signaling that in turn stabilizes Mcl-1. Indeed, injection of IL-6 in control mice resulted in marked phosphorylation of GSK-3β at S9 already 30 min postinjection, which was paralleled by increased Mcl-1 protein levels (Figure 3C). We then injected control and IL-6Rα^{KO} animals with 100 mg/kg DEN and assessed Mcl-1 stabilization and GSK-3β phosphorylation. While in control mice DEN injection stabilized Mcl-1 over time as a consequence of GSK-3β inactivation, this response was largely blunted in IL-6Rα^{KO} mice (Figure 3D). Mcl-1 stabilization as well as GSK-3β phosphorylation in controls corresponded with circulating IL-6 that peaked 8 hr upon injection (Figure S3F), whereas Mcl-1 stability was maintained up to 24 hr. However, PUMA peaked in both genotypes 24 hr after DEN injection on both the protein and RNA level, indicating that GSK-3β-independent mechanisms control *PUMA* expression in these experiments (Figures 3D and S3G). Thus, abrogation of IL-6 signaling results in decreased Mcl-1 protein stabilization during the early phases of DEN-induced liver tumorigenesis. To directly address the role of GSK-3β regarding Mcl-1 stabilization in vivo, we injected control mice with adeno-associated viral vectors (AAV) expressing either *GFP* or a Myc-tagged constitutive active GSK-3β variant (*GSK-3βCA*) harboring a serine-to-alanine substitution at position 9 of GSK-3β (S9A) (Figure 3E). Western blot analysis using Mcl-1 antibody demonstrated that expression of *GSK-3βCA* in livers of control mice reduced Mcl-1 protein level after DEN injection (Figure 3E), similarly to what was observed in IL-6Rα^{KO} animals (Figure 3D). In line with our previous experiment, *PUMA* expression failed to correlate with GSK-3β activity under acute DEN conditions, although we observed increased PUMA protein in noninjected *GSK-3βCA*-expressing livers (Figure 3E). These experiments therefore reveal that GSK-3β inactivation by phosphorylation at S9 is required during the initial phases of tumorigenesis to stabilize Mcl-1 protein levels.

GSK-3β S9 phosphorylation mainly occurs through the action of PI3K signaling (Cross et al., 1995). To determine the role of PI3K signaling in DEN-induced HCC development of HFD-fed mice, we treated HCC-bearing HFD fed control mice with the specific PI3K inhibitor GDC-0941. Accordingly, administration of GDC-0941 to tumor-bearing HFD fed mice resulted in reactivation of GSK-3β (Figure 3F). Consequently, Mcl-1 protein levels were reduced in the livers of these mice when compared to HFD-fed control mice, though livers of NCD fed IL-6Rα^{KO} mice still exhibited less Mcl-1 protein (Figure 3F). Furthermore, the reduction of Mcl-1 protein by inhibition of PI3K in tumor-bearing HFD fed control mice resulted in an increase of TUNEL-positive cells, a marker of apoptosis (Figures 3G and S3H). Moreover, Ki67 staining of tumor liver sections demonstrated that PI3K inhibition reduced hepatocyte proliferation (Figures 3H and S3I). Importantly, the quantitative evaluation of apoptosis and hepatocyte proliferation in livers of PI3K inhibitor-treated HFD fed control mice revealed a significant increase in apoptosis and reduction in proliferation comparable to that observed for NCD-fed IL-6Rα^{KO} mice, which are protected against HCC development. However, regardless of the result obtained from the pharmacological inhibition of PI3K, the formation of PIP_3 was similar in the cohorts of mice regardless of diet or genotype (Figure S3J).

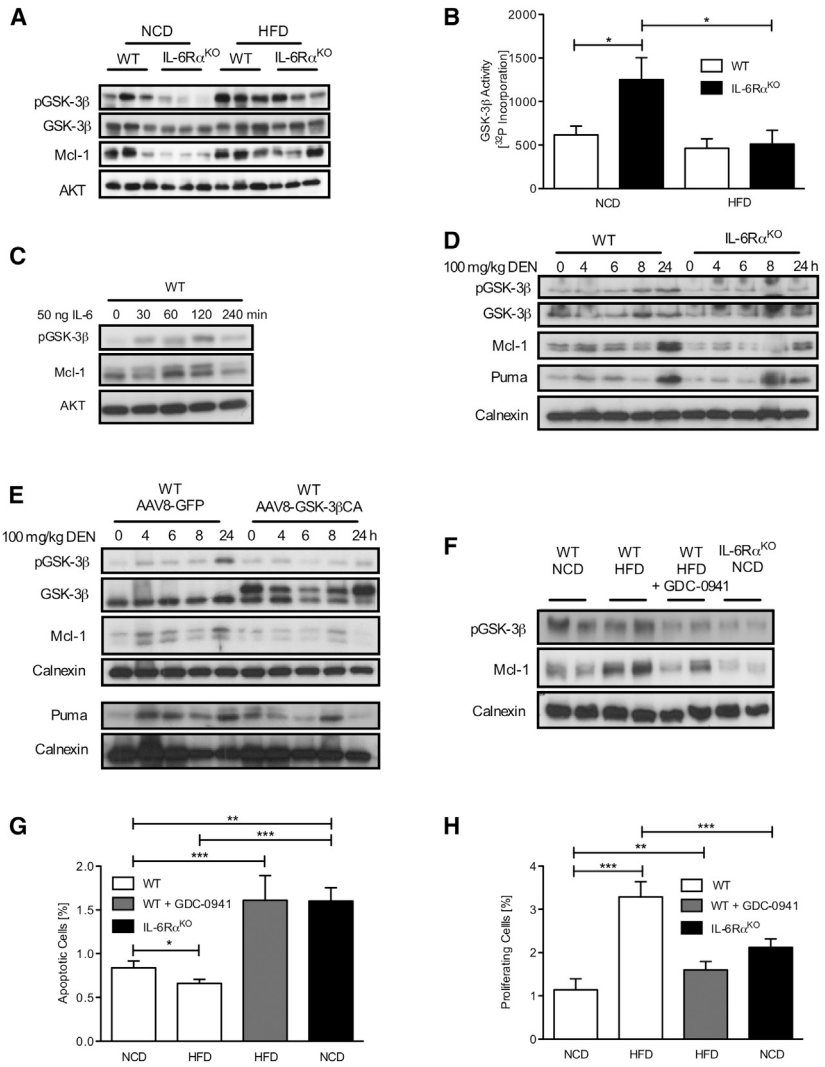

Figure 3. GSK-3β Inhibition Stabilizes Mcl-1 under Obese Conditions in HCC Development

(A) Western blot analysis using pGSK-3β, GSK-3β, Mcl-1, and AKT antibodies on liver tissue from DEN-injected 8-mo control and IL-6Rα^{KO} mice.

(B) Determination of GSK-3β activity in liver lysates from DEN-injected 8-mo control and IL-6Rα^{KO} mice (n = 5).

(C) Western blot analysis using pGSK-3β, Mcl-1, and AKT antibodies on liver tissue from 8-wk control mice fed on NCD after intravenous (i.v.) injection of 50 ng IL-6.

(D) Western blot analysis using pGSK-3β, GSK-3β, Mcl-1, PUMA, and Calnexin antibodies on liver tissue from 8-wk male control and IL-6Rα^{KO} mice fed on an NCD and sacrificed at the indicated time points after injection of 100 mg/kg DEN.

(E) Western blot analysis using pGSK-3β, GSK-3β, Mcl-1, PUMA, and Calnexin antibodies on liver tissue from 8-wk control mice preinfected with AAV8 viruses expressing *GFP* or *GSK-3βCA* at the indicated time points after injection of 100 mg/kg DEN.

(F) Western blot analysis using pGSK-3β, Mcl-1 and AKT antibodies on liver tissue from DEN-injected 8-mo control and IL-6Rα^{KO} mice treated with or without GDC-0941.

(G) Quantitation of apoptotic cells in tumor liver sections by TUNEL staining from DEN-injected 8-mo control and IL-6Rα^{KO} mice treated with or without GDC-0941 (n = 4).

(H) Quantitation of proliferating cells in tumor liver sections by Ki67 staining from DEN-injected 8-mo control and IL-6Rα^{KO} mice treated with or without GDC-0941 (n = 4).

Displayed values are means ± SEM; *p ≤ 0.05, **p ≤ 0.01, ***p ≤ 0.001 versus control. See also Figure S3.

Even downstream AKT activity was unaltered in those groups of mice as examined, on the one hand, by phosphorylation of AKT at serine 473 (Figures S3K and S3L) as well as by the ability of immunoprecipitated AKT to phosphorylate a GSK-3β S9 including peptide on the other (Figure S3M). Notably, these results are in discrepancy to the results obtained from whole-cell lysates (Figures 3A, 3B, S3A, and S3B). Thus, PI3K/AKT signaling is active, but not altered, in the absence of IL-6Rα signaling in HCC development independent on dietary condition.

Obesity and IL-6-Controlled Expression of *PP-1α* and *Mule* Synergize to Stabilize Mcl-1

Alteration of PI3K/AKT activity in lean *IL-6Rα*-deficient animals failed to explain increased GSK-3β action, so we examined the expression levels of protein phosphatase 1α (*PP-1α*), which catalyzes the reverse reaction, namely GSK-3β dephosphorylation at S9 (Figure 4A). Strikingly, expression levels of *PP-1α* were more than 2-fold increased in *IL-6Rα*-deficient mice in the DEN-induced HCC protocol when compared to controls (Figure 4A). Transcriptional control of IL-6-regulated gene expression is mainly mediated through the transcription factor Stat-3, whose activation was reduced in lean IL-6Rα^{KO} mice in acute as well as chronic DEN experiments (Figures S4A and S4B). Evidently, both the restored hepatic Stat-3 activation in obese IL-6Rα^{KO} mice and the remaining DEN-induced Stat-3 activation in lean IL-6Rα^{KO} mice occur independently of IL-6, thus indicating another obesity- and/or DEN-induced factor that activates Stat-3 in the absence of IL-6Rα (Figures S4A and S4B). Careful investigation of the *PP-1α* promoter revealed a conserved Stat-3 binding site between mice and humans upstream of transcriptional initiation (Figure S4C). To address whether this motif is bound by phosphorylated Stat-3 in response to IL-6, we performed chromatin immunoprecipitation (ChIP) experiments of basal and IL-6-stimulated HepG2 cells that demonstrated activated Stat-3 at this site under basal conditions but IL-6 stimulation increased the presence of Stat-3 at this motif (Figure 4B). To determine whether *PP-1α* is a direct IL-6 target in vivo and how expression is affected by IL-6-induced Stat-3 activation, we injected a cohort of C57/BL6 mice with IL-6 and examined relative hepatic expression of *PP-1α* in a time frame until 240 min after IL-6 injection (Figure 4C). *PP-1α* expression was significantly reduced upon IL-6

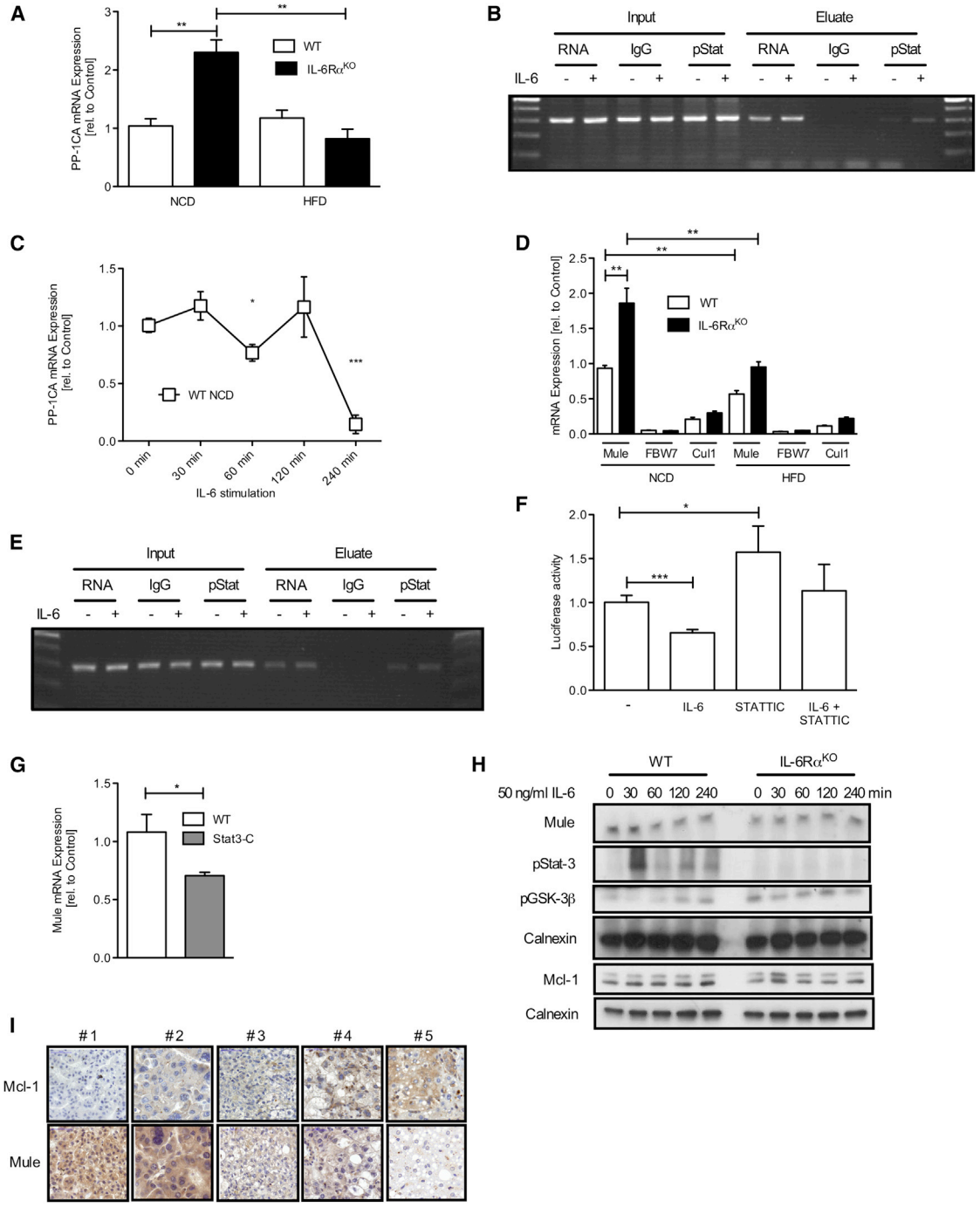

Figure 4. Obesity and IL-6-Controlled Expression of *PP-1α* and *Mule* Expression Synergize to Stabilize Mcl-1

(A) qPCR of *PP-1CA* in liver of DEN-injected 8-mo male control and IL-6Rα^{KO} mice fed on either NCD or HFD (n = 6).

(B) ChIP using RNA polymerase II, immunoglobulin G, and pStat-3 antibodies on sonicated DNA isolated from HepG2 cells stimulated with 200 ng/ml IL-6 for 45 min using oligos 5hPP1CAChip and 3hPP1CAChip to examine the *PP-1CA* promoter.

(C) qPCR of *PP-1CA* in liver of 8-wk control mice fed on NCD after i.v. injection of 50 ng IL-6 (n = 5).

(D) qPCR of *Mule*, *FBW7*, and *Cul1* in liver of DEN-injected 8-mo male control and IL-6Rα^{KO} mice (n = 6).

(E) ChIP using RNA polymerase II, immunoglobulin G, and pStat3 antibodies on sonicated DNA isolated from HepG2 cells stimulated with 200 ng/ml IL-6 for 45 min using oligos 5hMULEChip and 3hMULEChip to examine *Mule* promoter.

(F) Luciferase activity of lysates obtained from HepG2 cells transfected with pTEMule-Luc and pRL null stimulated with IL-6 and/or preincubated with 20μM STATTIC (n = 9/stimulation).

(G) qPCR of *Mule* in livers of 8-wk control and constitutive active Stat-3^{L-C} mice (n = 4).

(legend continued on next page)

treatment 60 min postinjection and progressively declined up to 240 min, indicating that *PP-1α* is a transcriptional target for IL-6-induced repression (Figure 4C). Noteworthy, IL-6-induced AKT activation already declined 60 min after injection (Figure S4D). To examine whether PP-1α inhibition is sufficient to stabilize Mcl-1 protein in acute DEN injection experiments in vivo, we applied the specific PP-1α inhibitor okadaic acid (OA) 1 hr before DEN injection in lean control and in *IL-6Rα*-deficient animals and investigated the S9 phosphorylation of GSK-3β as well as Mcl-1 protein abundance (Figure S4E). Expectedly, PP-1α inhibition resulted in the persistent phosphorylation of GSK-3β in both *IL-6Rα*-deficient and control mice (Figure S4E). However, hepatic Mcl-1 protein levels in *IL-6Rα*-deficient mice were still reduced when PP-1α was inhibited, hinting to another synergistic pathway independent of PP-1α and GSK-3β that destabilizes Mcl-1 in lean *IL-6Rα*-deficient mice. Of note, OA treatment in mice with liver-specific *GSK-3βCA* expression also reduced Mcl-1 protein levels (Figure S4F).

Recently, GSK-3β-phosphorylated Mcl-1 has been shown to be recognized by either Mule or the SCF^{FBW7} E3 ligase, both of which ligate polyubiquitin chains to Mcl-1 that lead to its proteasomal degradation (Wertz et al., 2011; Zhong et al., 2005). In order to determine whether the expression of these E3 ligases correlate with Mcl-1 levels in lean and obese control and *IL-6Rα*-deficient mice, we performed qPCR analyses of tumor livers from these mice (Figure 4D). Strikingly, while we observed a 2-fold elevated expression of *Mule* in lean *IL-6Rα*-deficient mice compared to lean controls, *Mule* expression was significantly reduced under obese conditions in mice of both genotypes (Figure 4D). Interestingly, comparing the expression levels of the subunits *FBW7* and *cullin 1* of the SCF^{FBW7} complex to *Mule* expression revealed a 20-fold lower *FBW7* expression and 5-fold lower *cullin 1* expression, indicating that Mule rather than the SCF^{FBW7} E3 ligase complex might play a role in liver carcinogenesis by interfering with Mcl-1 protein stability (Figure 4D). This result yielded the assumption that *Mule* expression is directly inhibited by IL-6 and that impaired suppression of *Mule* in *IL-6Rα*-deficient mice during HCC initiation and progression might result in increased Mcl-1 protein turnover and apoptosis. Consistently, examination of *Mule* expression in acute DEN injection experiments revealed that *IL-6Rα*-deficient mice showed an impaired suppression of *Mule* in response to DEN when compared to controls (Figure S4G). In line with these experiments that face to an important role of IL-6-induced Stat-3 in the inhibition of *Mule* expression, we analyzed the promoter region of *Mule* and identified two conserved Stat-3 binding motifs between mice and humans within a region upstream of *Mule* transcriptional initiation (Figure S4H). Chip experiments of basal and IL-6-stimulated HepG2 cells revealed active Stat-3 bound to the *Mule* promoter at the basal state, whereas IL-6 stimulation increased Stat-3 binding to these sites (Figure 4E). Of note, binding of activated Stat-3 to the Stat-3 motifs in the *Mule* promoter was specific, as using oligos more distal to these sites revealed still actively bound RNA polymerase II but not active Stat-3 (Figure S4I). To directly clarify whether *Mule* expression is subjected to IL-6-induced repression, we cloned 1,000 bp upstream of *Mule* exon 1 that contains the promoter including regulatory elements in front of a firefly luciferase and transfected this construct into HepG2 cells (Figure 4F). Examination of luciferase activity revealed significantly 40% reduced *Mule* promoter activity upon IL-6 stimulation, whereas luciferase activity substantially increased when transfected cells were incubated in the presence of the Stat-3 inhibitor STATTIC (Figure 4F). Accordingly, investigation of mice expressing a constitutive active Stat-3 variant in hepatocytes revealed a 40% reduced *Mule* expression similar to our in vitro findings (Figure 4G). Therefore, our analyses reveal that expression of the ubiquitin ligase *Mule* is directly regulated by IL-6- and obesity-controlled Stat-3 activation that impacts on Mcl-1 stability and thus alters apoptosis sensitivity.

In order to verify our mechanism of Mcl-1 stabilization in vitro, we stimulated primary hepatocytes derived from control and *IL-6Rα*-deficient animals with 50 ng/ml IL-6 in a time frame and performed western blot analysis (Figure 4H). This analysis revealed that IL-6 treatment increased Mcl-1 protein, inhibited GSK-3β activity, and repressed *Mule* expression in control hepatocytes, whereas these processes were not present in *IL-6Rα*-deficient cells (Figure 4H). Notably, these experiments also demonstrate that our mechanism of IL-6-induced Mcl-1 stabilization is more pronounced in vivo that might point to an auxiliary function for IL-6 in liver nonparenchymal cells. IL-6 signaling in these cells might in turn promote hepatic Mcl-1 stabilization through other indirect means. Nevertheless, we verified our in vivo mechanism of IL-6-induced Mcl-1 stabilization in primary hepatocytes, although IL-6 action in vivo is more effective to stabilize Mcl-1.

Increased Mcl-1 levels have previously been reported in a subset of human HCC (Fleischer et al., 2006); however, the correlation between Mcl-1 and Mule has never been addressed in HCC. Therefore, we examined human HCC samples in immunohistochemistry using anti-Mule and anti-Mcl-1 antibodies, revealing that *Mcl-1* expression in human HCC negatively correlated with *Mule* expression (Figure 4I). We classified cases that showed no steatosis (#1 and #2), steatosis (#3), and a steatohepatitic pattern (#4 and #5) by visible lipid inclusions into the liver. While, the nonsteatotic cases #1 and #2 showed almost no *Mcl-1* expression and high *Mule* expression, the steatohepatitic HCC cases #4 and #5 exhibited the most prominent *Mcl-1* expression accompanied with a reduction in *Mule* expression, implicating our experiments as truly translational and ominous in light of the steadily increasing obesity epidemic. Collectively, our experiments demonstrate that obesity and IL-6 signaling synergize to affect the protein stability of the Bcl-2 family member Mcl-1 via GSK-3β inhibition and repression of *Mule* expression to inhibit the mitochondrial apoptotic pathway during HCC development.

(H) Western blot analysis using pStat-3, Mcl-1, AKT, Mule, pGSK-3β, and Calnexin antibodies of primary hepatocytes derived from control and $IL\text{-}6R\alpha^{KO}$ mice stimulated with 50 ng/ml IL-6 for the indicated time points.
(I) Mcl-1 and Mule stainings of five different human HCC sections.
Displayed values are means ± SEM; *$p \leq 0.05$, **$p \leq 0.01$, ***$p \leq 0.001$ versus control. See also Figure S4.

DISCUSSION

The current obesity epidemic in westernized societies represents a major health burden owing to the development of obesity-associated diseases. The excessive weight gain in obesity is accompanied with a chronic inflammatory state mainly derived from obese WAT that releases TNF-α and IL-6 into the bloodstream (Xu et al., 2003). Interestingly, epidemiological studies identified HCC as a cancer entity, the risk of which is clearly increased in obese subjects, particularly in men with a body mass index of more than 35 (Calle et al., 2003). However, the impact of obesity-induced low-grade inflammation on the development of neoplastic lesions has not yet been studied in detail.

Importantly, the enhanced development and progression of HCC in obesity can be recapitulated in mouse models for HCC to elucidate the underlying molecular mechanisms of obesity-induced HCC development (Park et al., 2010; Wunderlich et al., 2008). Recently, Park et al. (2010) demonstrated that both dietary- and genetically induced obesity in mice increase HCC development as a consequence of obesity-induced elevation of both TNF-α and IL-6. In this context, increased IL-6 levels in obesity were predicted to inhibit hepatocyte apoptosis, a driving force in DEN-induced HCC development. Our study has now identified that stabilization of Mcl-1 is the molecular basis for IL-6-induced protection from apoptosis in lean mice. Along this line, previous studies have clearly demonstrated that Mcl-1 is an antiapoptotic factor for a subset of human HCC, whose inhibition might have potential in human therapy (Fleischer et al., 2006; Schulze-Bergkamen et al., 2006), but may also result in liver damage and cancer development (Vick et al., 2009; Weber et al., 2010). It has been previously demonstrated that hepatocyte-specific *Mcl-1* inactivation causes spontaneous HCC in old mice as a consequence of a microenvironment comprising apoptosis-sensitive *Mcl-1*-deficient hepatocytes and compensating adjacent hepatocytes (Weber et al., 2010). Of note, HCC development in these mice occurs in the absence of chronic inflammation. Interestingly, the compound inactivation of *Mcl-1* and *BAK* not only normalizes apoptosis sensitivity of hepatocytes but also prevents liver cancer development (Hikita et al., 2012). However, the *Mcl-1*-deficient mouse model of liver cancer is different from our DEN-induced HCC model, which depends on high Mcl-1 levels that are translatable to human disease (Fleischer et al., 2006) and where IL-6 action stabilizes Mcl-1 protein through inhibition of posttranslational mechanisms. Of note is that unlike other Bcl-2 family members, Mcl-1 has a dynamic turnover rate (Kozopas et al., 1993; Maurer et al., 2006). While *Mcl-1* expression at the transcriptional level depends on PI3K-mediated signal transduction as well as IL-6-evoked signaling (Epling-Burnette et al., 2001; Jourdan et al., 2003; Wang et al., 1999), the dynamic turnover rate of Mcl-1 is controlled by GSK-3β phosphorylation leading to its polyubiquitylation and subsequent proteasome-mediated degradation (Maurer et al., 2006). The regulation of GSK-3β is complex and controlled at multiple levels and its misregulation is known to contribute to the development of numerous diseases such as diabetes, Alzheimer disease, and cancer (Eldar-Finkelman and Krebs, 1997; Eldar-Finkelman et al., 1999; Hanger et al., 1992; Patel and Woodgett, 2008). While S9 in GSK-3β is mainly a substrate for AKT phosphorylation in response to insulin (Cross et al., 1995), phosphorylation of this site can also be catalyzed by PKA or PKC (Fang et al., 2000, 2002; Wang et al., 1994). Whatever the nature of the upstream kinase that controls GSK-3β phosphorylation, our experiments reveal that its activity in HCC is controlled via both the activation of PI3K signaling and PP-1α that catalyzes the removal of S9 phosphorylation. While we clearly demonstrate that PI3K/AKT action is not impaired in the absence of IL-6Rα signaling, our experiments reveal a critical role of IL-6 signaling in the control of *PP-1α* expression. However, while S9 phosphorylation-dependent control of GSK-3β kinase activity was shown to regulate Mcl-1 protein stability, GSK-3β action requires prephosphorylation of Mcl-1 in order to exert its regulatory function (Maurer et al., 2006; Morel et al., 2009). Nevertheless, we found in our mouse model that GSK-3β phosphorylation correlated with Mcl-1 protein stability. However, at this point we cannot rule out that depending on dietary conditions IL-6Rα signaling in addition to GSK-3β regulation also controls the activity of additional Mcl-1 kinases. In line with this notion, previous studies have suggested that MAPK/ERK and JNK-dependent phosphorylation of Mcl-1 may also decrease Mcl-1 stability (Domina et al., 2004; Kodama et al., 2009; Morel et al., 2009). Further, increased and sustained JNK-1 activity, as observed in obesity (Hirosumi et al., 2002) and during DEN-induced HCC development (Hui et al., 2008), can stabilize Mcl-1 (Kodama et al., 2009).

The protein stability of Mcl-1 critically depends on the action of E3 ubiquitin ligases that polyubiquitylate Mcl-1 leading to its proteosomal degradation. In particular, the SCF^{FBW7} complex and Mule have been described in this context (Wertz et al., 2011; Zhong et al., 2005). While we detected only marginal expression of the subunits *FBW7* and *cullin-1* in HCC, we demonstrate that *Mule* expression is a direct target of IL-6-mediated Stat-3 repression and that in human HCC, Mcl-1 levels negatively correlate with *Mule* expression. Thus, in lean mice, IL-6 exaggerates Mcl-1 stabilization in HCC by controlling the synergistic actions of GSK-3β and Mule. In contrast, in obesity, DEN-induced HCC development and progression occurred even in the absence of *IL-6Rα* expression as a consequence of obesity-induced GSK-3β inhibition and transcriptional repression of *Mule* leading to Mcl-1 stabilization. Along these lines, inhibitory S9 phosphorylation of GSK-3β was increased upon HFD feeding both in control and $IL\text{-}6R\alpha^{KO}$ mice, whereas *Mule* expression was significantly inhibited under obese conditions not only in control but also in *IL-6Rα*-deficient animals. Therefore in lean mice, IL-6 appears to be the critical regulator of GSK-3β as well as *Mule* inhibition, while alternative signals may control these molecules in obese mice. Interestingly, while the increased tumor burden in obese mice was accompanied with increased Mcl-1 levels in tumor lesions independently of IL-6Rα signaling, the severity of tumor-specific lipid accumulation in human HCC positively correlated with Mcl-1 abundance. Apparently, our experiments refer to a not-yet-identified factor that compensates for *IL-6Rα* deficiency in obesity-associated HCC development. We have good indication that another IL-6-type cytokine or receptor might represent this obesity-induced factor as inactivation of *gp130* in hepatocytes protects against DEN-induced

HCC development even under obese conditions. We propose that this factor is increased also in the proinflammatory state in obesity, thereby elevating basal hepatic Stat-3 activation but impairing acute factor-induced responsiveness. Indeed, we have demonstrated such characteristics for IL-6 under obese conditions. While the identification of the obesity-induced factor that stabilizes Mcl-1 might open novel avenues to treat human HCC, it would clarify another interesting aspect of our study, namely the apparent differential effect of predescribed *IL-6* deficiency versus our results on *IL-6Rα* deficiency in obesity-induced HCC development. Both *IL-6* and *IL-6Rα* deficiency in lean mice protect against HCC development, whereas in the obese state, IL-6Rα^{KO} mice exhibit similar tumor numbers as control mice but *IL-6* knockout mice fail to develop HCC under these conditions (Park et al., 2010). In line with these reported differential effects, a recent publication demonstrated a similarly different experimental outcome in *IL-6*- and *IL-6Rα*-deficient mice when addressing the function of IL-6 in wound healing (McFarland-Mancini et al., 2010). While *IL-6*-deficient mice demonstrated a greatly reduced wound-healing capacity, *IL-6Rα* deficiency showed only slightly impaired wound healing. Further analysis of double-knockout mice revealed that *IL-6Rα* deficiency dominated wound-healing capacity. Thus, these studies and our latest findings point toward a more complex role of IL-6Rα signaling in inflammatory processes than hitherto assumed. Collectively, our study has clearly identified IL-6- and obesity-induced Mcl-1 stabilization as a critical factor for HCC development and progression. Moreover, our study provides evidence that under obese conditions, IL-6Rα-dependent regulation of GSK-3β and *Mule* is compensated for by an alternative mechanism. Thus, this study has strong implications for current translational research on HCC and the development of novel therapeutic strategies aiming at reactivating the mitochondrial apoptotic pathway under inflammatory and obese conditions.

EXPERIMENTAL PROCEDURES

Care of all animals was within institutional animal care committee guidelines and all animal procedures were approved by local government authorities (Bezirksregierung Köln, Cologne, Germany) and were in accordance with NIH guidelines. Experimental procedures are described in detail in the Extended Experimental Procedures.

SUPPLEMENTAL INFORMATION

Supplemental Information includes Extended Experimental Procedures and four figures and can be found with this article online at http://dx.doi.org/10.1016/j.celrep.2013.07.023.

ACKNOWLEDGMENTS

This work was supported by the DFG through grants SFB 832 A15 (to F.T.W.) and Z3 (to J.C.B.), the Center for Molecular Medicine (CMMC) (grants D1 to J.C.B., B2 to F.T.W., and B1 to H.B.), the Cluster of Excellence Cellular Stress Responses in Aging-Associated Diseases (CECAD), the European Union (grant FP7-HEALTH-2009-241592, EurOCHIP, to J.C.B.), the DFG (grant BR 1492/7-1 to J.C.B.), and the Competence Network for Adipositas (Neurotarget) funded by the Federal Ministry of Education and Research (grant FKZ01GIO845 to J.C.B.). This work was in part funded by grants of the DFG to B.K.S. (STR 1160/1-1) and to P.S. (SFB-TRR7, project B5) and by the CRC 670 to H.B. We thank Brigitte Hampel, Anke Lietzau, Cathy Baitzel, Hanna Janicki, Sarah Meßnard, and Elisabeth Specht for expert technical assistance and Jude Samulski and James Wilson for providing pXX6-80 and pXR8, respectively.

Received: December 20, 2012
Revised: April 19, 2013
Accepted: July 17, 2013
Published: August 15, 2013

REFERENCES

Bianchini, F., Kaaks, R., and Vainio, H. (2002). Overweight, obesity, and cancer risk. Lancet Oncol. *3*, 565–574.

Bisgaard, H.C., and Thorgeirsson, S.S. (1996). Hepatic regeneration. The role of regeneration in pathogenesis of chronic liver diseases. Clin. Lab. Med. *16*, 325–339.

Brunelle, J.K., and Letai, A. (2009). Control of mitochondrial apoptosis by the Bcl-2 family. J. Cell Sci. *122*, 437–441.

Calle, E.E., and Kaaks, R. (2004). Overweight, obesity and cancer: epidemiological evidence and proposed mechanisms. Nat. Rev. Cancer *4*, 579–591.

Calle, E.E., Rodriguez, C., Walker-Thurmond, K., and Thun, M.J. (2003). Overweight, obesity, and mortality from cancer in a prospectively studied cohort of U.S. adults. N. Engl. J. Med. *348*, 1625–1638.

Charvet, C., Wissler, M., Brauns-Schubert, P., Wang, S.J., Tang, Y., Sigloch, F.C., Mellert, H., Brandenburg, M., Lindner, S.E., Breit, B., et al. (2011). Phosphorylation of Tip60 by GSK-3 determines the induction of PUMA and apoptosis by p53. Mol. Cell *42*, 584–596.

Cross, D.A., Alessi, D.R., Cohen, P., Andjelkovich, M., and Hemmings, B.A. (1995). Inhibition of glycogen synthase kinase-3 by insulin mediated by protein kinase B. Nature *378*, 785–789.

Ding, Q., He, X., Hsu, J.M., Xia, W., Chen, C.T., Li, L.Y., Lee, D.F., Liu, J.C., Zhong, Q., Wang, X., and Hung, M.C. (2007). Degradation of Mcl-1 by beta-TrCP mediates glycogen synthase kinase 3-induced tumor suppression and chemosensitization. Mol. Cell. Biol. *27*, 4006–4017.

Domina, A.M., Vrana, J.A., Gregory, M.A., Hann, S.R., and Craig, R.W. (2004). MCL1 is phosphorylated in the PEST region and stabilized upon ERK activation in viable cells, and at additional sites with cytotoxic okadaic acid or taxol. Oncogene *23*, 5301–5315.

Eldar-Finkelman, H., and Krebs, E.G. (1997). Phosphorylation of insulin receptor substrate 1 by glycogen synthase kinase 3 impairs insulin action. Proc. Natl. Acad. Sci. USA *94*, 9660–9664.

Eldar-Finkelman, H., Schreyer, S.A., Shinohara, M.M., LeBoeuf, R.C., and Krebs, E.G. (1999). Increased glycogen synthase kinase-3 activity in diabetes- and obesity-prone C57BL/6J mice. Diabetes *48*, 1662–1666.

Epling-Burnette, P.K., Liu, J.H., Catlett-Falcone, R., Turkson, J., Oshiro, M., Kothapalli, R., Li, Y., Wang, J.M., Yang-Yen, H.F., Karras, J., et al. (2001). Inhibition of STAT3 signaling leads to apoptosis of leukemic large granular lymphocytes and decreased Mcl-1 expression. J. Clin. Invest. *107*, 351–362.

Fang, X., Yu, S.X., Lu, Y., Bast, R.C., Jr., Woodgett, J.R., and Mills, G.B. (2000). Phosphorylation and inactivation of glycogen synthase kinase 3 by protein kinase A. Proc. Natl. Acad. Sci. USA *97*, 11960–11965.

Fang, X., Yu, S., Tanyi, J.L., Lu, Y., Woodgett, J.R., and Mills, G.B. (2002). Convergence of multiple signaling cascades at glycogen synthase kinase 3: Edg receptor-mediated phosphorylation and inactivation by lysophosphatidic acid through a protein kinase C-dependent intracellular pathway. Mol. Cell. Biol. *22*, 2099–2110.

Fleischer, B., Schulze-Bergkamen, H., Schuchmann, M., Weber, A., Biesterfeld, S., Müller, M., Krammer, P.H., and Galle, P.R. (2006). Mcl-1 is an anti-apoptotic factor for human hepatocellular carcinoma. Int. J. Oncol. *28*, 25–32.

Ford, E.S., and Mokdad, A.H. (2008). Epidemiology of obesity in the Western Hemisphere. J. Clin. Endocrinol. Metab. *93*(11, Suppl 1), S1–S8.

Hanger, D.P., Hughes, K., Woodgett, J.R., Brion, J.P., and Anderton, B.H. (1992). Glycogen synthase kinase-3 induces Alzheimer's disease-like phosphorylation of tau: generation of paired helical filament epitopes and neuronal localisation of the kinase. Neurosci. Lett. *147*, 58–62.

Heinrich, P.C., Behrmann, I., Haan, S., Hermanns, H.M., Müller-Newen, G., and Schaper, F. (2003). Principles of interleukin (IL)-6-type cytokine signalling and its regulation. Biochem. J. *374*, 1–20.

Hikita, H., Kodama, T., Shimizu, S., Li, W., Shigekawa, M., Tanaka, S., Hosui, A., Miyagi, T., Tatsumi, T., Kanto, T., et al. (2012). Bak deficiency inhibits liver carcinogenesis: a causal link between apoptosis and carcinogenesis. J. Hepatol. *57*, 92–100.

Hirosumi, J., Tuncman, G., Chang, L., Görgün, C.Z., Uysal, K.T., Maeda, K., Karin, M., and Hotamisligil, G.S. (2002). A central role for JNK in obesity and insulin resistance. Nature *420*, 333–336.

Hotamisligil, G.S. (2006). Inflammation and metabolic disorders. Nature *444*, 860–867.

Hui, L., Zatloukal, K., Scheuch, H., Stepniak, E., and Wagner, E.F. (2008). Proliferation of human HCC cells and chemically induced mouse liver cancers requires JNK1-dependent p21 downregulation. J. Clin. Invest. *118*, 3943–3953.

Jourdan, M., Veyrune, J.L., De Vos, J., Redal, N., Couderc, G., and Klein, B. (2003). A major role for Mcl-1 antiapoptotic protein in the IL-6-induced survival of human myeloma cells. Oncogene *22*, 2950–2959.

Kodama, Y., Taura, K., Miura, K., Schnabl, B., Osawa, Y., and Brenner, D.A. (2009). Antiapoptotic effect of c-Jun N-terminal Kinase-1 through Mcl-1 stabilization in TNF-induced hepatocyte apoptosis. Gastroenterology *136*, 1423–1434.

Kozopas, K.M., Yang, T., Buchan, H.L., Zhou, P., and Craig, R.W. (1993). MCL1, a gene expressed in programmed myeloid cell differentiation, has sequence similarity to BCL2. Proc. Natl. Acad. Sci. USA *90*, 3516–3520.

Luedde, T., Beraza, N., Kotsikoris, V., van Loo, G., Nenci, A., De Vos, R., Roskams, T., Trautwein, C., and Pasparakis, M. (2007). Deletion of NEMO/IKKgamma in liver parenchymal cells causes steatohepatitis and hepatocellular carcinoma. Cancer Cell *11*, 119–132.

Maurer, U., Charvet, C., Wagman, A.S., Dejardin, E., and Green, D.R. (2006). Glycogen synthase kinase-3 regulates mitochondrial outer membrane permeabilization and apoptosis by destabilization of MCL-1. Mol. Cell *21*, 749–760.

McFarland-Mancini, M.M., Funk, H.M., Paluch, A.M., Zhou, M., Giridhar, P.V., Mercer, C.A., Kozma, S.C., and Drew, A.F. (2010). Differences in wound healing in mice with deficiency of IL-6 versus IL-6 receptor. J. Immunol. *184*, 7219–7228.

Morel, C., Carlson, S.M., White, F.M., and Davis, R.J. (2009). Mcl-1 integrates the opposing actions of signaling pathways that mediate survival and apoptosis. Mol. Cell. Biol. *29*, 3845–3852.

Naugler, W.E., Sakurai, T., Kim, S., Maeda, S., Kim, K., Elsharkawy, A.M., and Karin, M. (2007). Gender disparity in liver cancer due to sex differences in MyD88-dependent IL-6 production. Science *317*, 121–124.

Nishimura, S., Manabe, I., Nagasaki, M., Eto, K., Yamashita, H., Ohsugi, M., Otsu, M., Hara, K., Ueki, K., Sugiura, S., et al. (2009). CD8+ effector T cells contribute to macrophage recruitment and adipose tissue inflammation in obesity. Nat. Med. *15*, 914–920.

Park, E.J., Lee, J.H., Yu, G.Y., He, G., Ali, S.R., Holzer, R.G., Osterreicher, C.H., Takahashi, H., and Karin, M. (2010). Dietary and genetic obesity promote liver inflammation and tumorigenesis by enhancing IL-6 and TNF expression. Cell *140*, 197–208.

Patel, S., and Woodgett, J. (2008). Glycogen synthase kinase-3 and cancer: good cop, bad cop? Cancer Cell *14*, 351–353.

Schulze-Bergkamen, H., Fleischer, B., Schuchmann, M., Weber, A., Weinmann, A., Krammer, P.H., and Galle, P.R. (2006). Suppression of Mcl-1 via RNA interference sensitizes human hepatocellular carcinoma cells towards apoptosis induction. BMC Cancer *6*, 232.

Vick, B., Weber, A., Urbanik, T., Maass, T., Teufel, A., Krammer, P.H., Opferman, J.T., Schuchmann, M., Galle, P.R., and Schulze-Bergkamen, H. (2009). Knockout of myeloid cell leukemia-1 induces liver damage and increases apoptosis susceptibility of murine hepatocytes. Hepatology *49*, 627–636.

Wang, Q.M., Fiol, C.J., DePaoli-Roach, A.A., and Roach, P.J. (1994). Glycogen synthase kinase-3 beta is a dual specificity kinase differentially regulated by tyrosine and serine/threonine phosphorylation. J. Biol. Chem. *269*, 14566–14574.

Wang, J.M., Chao, J.R., Chen, W., Kuo, M.L., Yen, J.J., and Yang-Yen, H.F. (1999). The antiapoptotic gene mcl-1 is up-regulated by the phosphatidylinositol 3-kinase/Akt signaling pathway through a transcription factor complex containing CREB. Mol. Cell. Biol. *19*, 6195–6206.

Weber, A., Boger, R., Vick, B., Urbanik, T., Haybaeck, J., Zoller, S., Teufel, A., Krammer, P.H., Opferman, J.T., Galle, P.R., et al. (2010). Hepatocyte-specific deletion of the antiapoptotic protein myeloid cell leukemia-1 triggers proliferation and hepatocarcinogenesis in mice. Hepatology *51*, 1226–1236.

Wertz, I.E., Kusam, S., Lam, C., Okamoto, T., Sandoval, W., Anderson, D.J., Helgason, E., Ernst, J.A., Eby, M., Liu, J., et al. (2011). Sensitivity to antitubulin chemotherapeutics is regulated by MCL1 and FBW7. Nature *471*, 110–114.

Wunderlich, F.T., Luedde, T., Singer, S., Schmidt-Supprian, M., Baumgartl, J., Schirmacher, P., Pasparakis, M., and Brüning, J.C. (2008). Hepatic NF-kappa B essential modulator deficiency prevents obesity-induced insulin resistance but synergizes with high-fat feeding in tumorigenesis. Proc. Natl. Acad. Sci. USA *105*, 1297–1302.

Wunderlich, F.T., Ströhle, P., Könner, A.C., Gruber, S., Tovar, S., Brönneke, H.S., Juntti-Berggren, L., Li, L.S., van Rooijen, N., Libert, C., et al. (2010). Interleukin-6 signaling in liver-parenchymal cells suppresses hepatic inflammation and improves systemic insulin action. Cell Metab. *12*, 237–249.

Wunderlich, C.M., Delic, D., Behnke, K., Meryk, A., Strohle, P., Chaurasia, B., Al-Quraishy, S., Wunderlich, F., Bruning, J.C., and Wunderlich, F.T. (2012). Cutting edge: Inhibition of IL-6 trans-signaling protects from malaria-induced lethality in mice. J Immunol *188*, 4141–4144.

Xu, H., Barnes, G.T., Yang, Q., Tan, G., Yang, D., Chou, C.J., Sole, J., Nichols, A., Ross, J.S., Tartaglia, L.A., and Chen, H. (2003). Chronic inflammation in fat plays a crucial role in the development of obesity-related insulin resistance. J. Clin. Invest. *112*, 1821–1830.

Zhong, Q., Gao, W., Du, F., and Wang, X. (2005). Mule/ARF-BP1, a BH3-only E3 ubiquitin ligase, catalyzes the polyubiquitination of Mcl-1 and regulates apoptosis. Cell *121*, 1085–1095.